MINAR International Journal of Applied Sciences and Technology

Article type : Research Article

Date Received : 02/04/2021
Date Accepted : 26/04/2021
Date published : 01/06/2021
: www.minarjournal.com
http://dx.doi.org/10.47832/2717-8234.2-3.7

COMPARISON STUDY BETWEEN SPECTROSCOPIC ANALYSIS FOR (ZN,SN) PLASMA BY LIBS

Hadeel K. NASIF[1], Kadhim A. AADIM [2]& Baida M. AHMED[3]

Abstract

This article a spectroscopic research on laser-produced Tin and Zinc plasmas using the optical emission spectroscopy (OES) technique. Plasmas can be produced from a solid tin and zinc targets irradiated with a pulsed laser in room environments. The spectrum is recorded for the Sn, Zn laser plasma Nd: YAG with a wavelength of (1064) nm, a duration of (9) ns, and a frequency of (6) Hz and a focal length of (10) cm within the energy range (300-800)mj. By using the ratio line strength formula, the electron temperature (Te) can be calculated and the result is for Zinc (Zn) plasma (2.11 ev) and tin (Sn) plasma (1,227 ev). The Saha-Boltzmann equation will be used to calculate electron density (ne) in this method and the values for zinc (Zn) (3.3 cm-3)and tin (Sn) (2.1 cm-3). The plasma parameters, such as plasma (fp), Debye duration (λD), and Debye number (ND), were calculated in the proposed document.

Keywords: Spectroscopy, LIBS, plasma parameters, Tin(Sn), Zinc(Zn).

[1] Mustansiriyah University, Iraq, hadellkhaled1991@yahoo.com, https://orcid.org/0000-0001-7368-1685
[2] Baghdad University, Iraq, kadhim_adem@scbaghdad.edu.iq, https://orcid.org/0000-0003-4533-5309
[3] Mustansiriyah University, Iraq, baida_222@yahoo.com, https://orcid.org/0000-0001-9315-1913

1. Introduction

Laser Induced Breakdown Spectroscopy [LIBS] is a common tool for supporting precise quantitative physical analysis in situ . As the excitation source, it utilizes a high energy laser pulse . It can be used to analyze any substance, such as gas, solid or liquid, regardless of its physical stateWith the aid of its laser mediated plasma emission signals, it tracks certain atomic and molecular species[1]. This works on the surface of the target material with the laser beam and produces the plasma . In this process, the laser beam excites and ionizes the target material The plasma emission will begin on the target surface of the material as soon as the laser photon reaches the target surface . The laser-induced plasma emission spectra can detect atomic and molecular species for optical application. The collection of experimental conditions affects LIBS empirical outcomes. LIBS output is affected by laser pulse energy, pulse rate, observation time rate, atmospheric gas pressure, target type, properties of the target material, geometric configuration of optical instruments [2,3]. Such parameters have a major impact on LIBS efficiency. Driven pulsed solid laser plasma plays a crucial role in laboratory astrophysics, applied sciences, x-ray laser plasma sources [4]. Latest analysis has shown that LIBS has been used to analyze biological samples such as tissues, diverse forms of bacteria, gall stones and aerosols . Laser-induced plasmas [LIP] are used as spectroscopic sources to gain substantial benefits [5,6,7]. The important effect on optical emission spectroscopy is seen by LIP. The prevailing technique to produce the plasma electronically from the plasma aroused species is considered[8]. The optical radiation spectrum using the ratio principle is one of the characteristics of the LIPS Basically, it is used to measure electron temperature and density . In this process the energy of the electrons are distinguished[9]. The thermodynamic equilibrium equation defines the plasma temperature with (LTE) [10] .

$$T = \frac{-(E_1 - E_2)}{k \ln\left(\frac{I_1 \lambda_1 A_2 g_2}{I_2 \lambda_2 A_1 g_1}\right)} \quad (1)$$

in represent equation the intensity, is referred by the intensity I1, I2 and g is the statistical weight.
Equation 2 g is the statistical weight. λ is a wavelength, A is referred as the probability of transition. K is the Boltzmann Continuous factor. E1 and E2 are referred as the excited state energy values in eV., The number of free electrons per unit volume are determined by the electron density. The equation is developed from the principles of BotzmannSaha , spectral lines of the same element and successive stages of ionization [11].

$$n_e = \frac{I_1}{I_2^*} 6.04 \times 10^{21} (T)^{3/2} e^{\frac{(E_1 - E_2 - X_z)}{kT}} \quad (2)$$

Equation 2 is representing the transition wavelength from level (2) to level (1) n_e is thedensity of electron, X_z is the ionizing energy eV .
where:

$$I_2^* = \frac{I_2 \lambda_2}{g_2 A_2} \quad (3)$$

In the above equation g_2 are the transition statistical weitht from level (2) to Level (1). A_2 is represente the transition probability from level (2) to Level (1). The plasma frequency can be obtained from the following equation [12].

$$f_p = \sqrt{\frac{e^2 n_e}{m_e \varepsilon_o}} \quad (4)$$

The frequency is dependent on the plasma density. One of the most important plasma parameters is plasma frequency [12]. Debye length the important function of plasma. The distance is reflecting the charged particle which is going to impact on individual particle. It brings a reverse charge within the plasma medium. The Electron mass m_e , ε_o the permittivity the Debye length λ_D It is proportional equalent to the square root of the temperature Te of the electron and inversely to the density ne of the electron according to [13].

$$\lambda_D = \sqrt{\frac{\varepsilon o \, K_B \, Te}{ne \, q2e}} \cong 7430 * \left(\frac{T_e}{ne}\right)^{1/2} \quad (5)$$

In the above equation ne represent the density of the electron. T_e represents the temperature of electron and q_2e represents the electron charge. The number of particles in the Debye sphere are represented by N_D. It is proportionate to electron density and electron temperature. It is also representing the second condition for plasma existence. N_D>>1[14].

$$N_D = \frac{4}{3}\pi\lambda_D^3 n_e \quad (6)$$

2-Experiment details

The experiment is performed on solid targets for Sn and Zn by using pulsed laser. This method produced the plasma. It is achieved using [LIPS] laser induced plasma spectroscopy. The laboratory structure for using LIPS is shown in Figure-1 below.

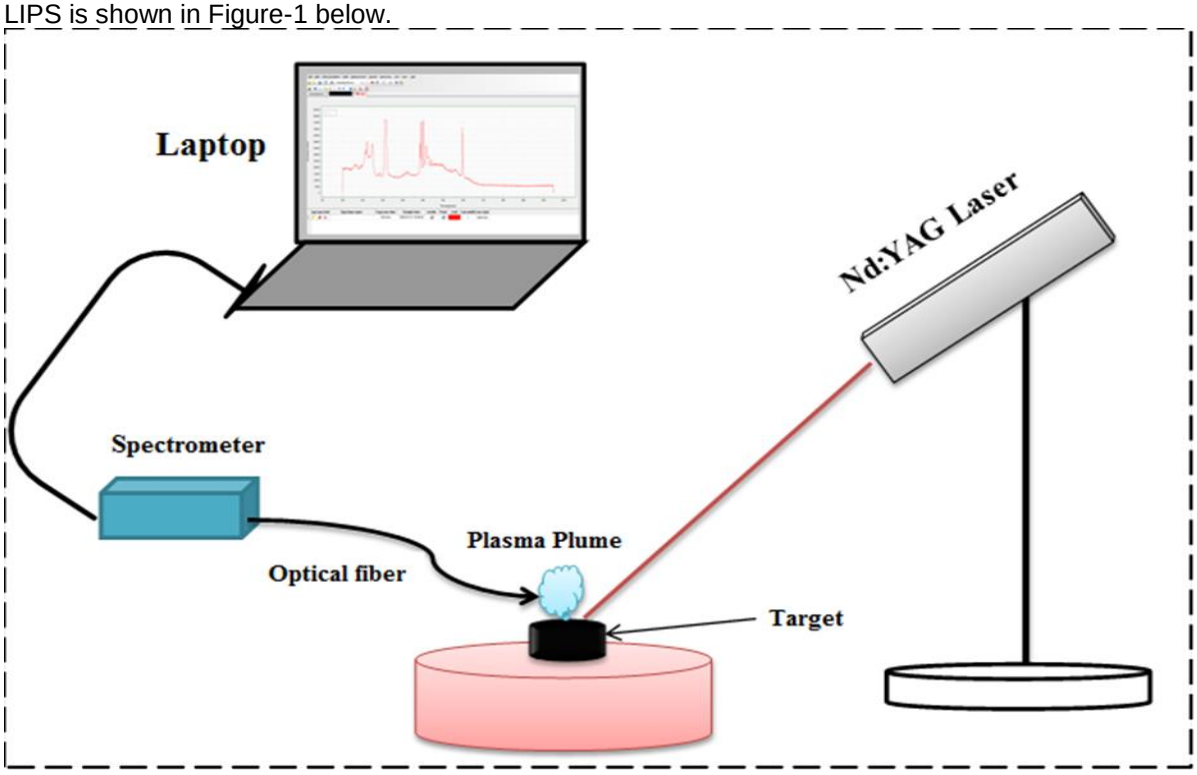

Fig -1 Laboratory arrangement for LIPS setup

The plasma is produced in this experiment by a Q-switched pulsed laser Nd: YAG with a wavelength of 1064 nm and a frequency of 6 Hz . Q-Switch delay via laser controller is used in this phase to streak light . Pulse laser energy is transmitted by the energy meter and measured . The pulse of a laser is created by the arrangement of the operating 450 angles .The laser beam hits material which evaporates and ionizes the substance formulate the plasma plume on the surface of the targeted material . The functional emission spectroscopy method is used to distinguish the electron temperature, density and frequency of this method The mathematically measured length of Debye was. The spectrometer enriches this operation In each fired, spectrometers are primarily used. The Surwit [S3000-UV-NIR] spectrometer is used in this experiment to test the system's emission wavelength (200-1000) and high-performance throughput [15].

3-Results and Discussion

3-1 Influence of Laser Energy on the Emission Spectrum

The effect of pulse laser energy on the emission spectrum of Sn and Zn plasmas at (200-1000) nm wavelength range has been studied in more detail in this section.

3-1-1 Sn plasma

Figure-2 displays the emission spectrum of Sn plasma from varying laser energies at ambient air pressure.Many properties can be seen in this figure that there are many neutral Tin (Sn I) peaks in the

spectrum at wavelengths between 284.5 , 303.66 , 713.73 , 326.1 , 334.73 , 380.53 and 452.84 nm.The Sn II ionic emission lines also occur at 533.73 , 558.88 , 580.2 , 645.39 , 684.4 , 719.5 and 777.25 nm wavelengths.The amplitude of both peaks increases as laser energy increases.Moreover, based on the findings shown in Figure-2, the overall emission line strength of Sn I is much higher than that of Sn II.These findings suggested that the produced plasma contained more atomic Sn than ionic Sn.This reality can be clarified as the ionization processes occur a very short period of less than a millisecond before atomization, according to the plasma generation process.Thus, by the recombination process, the electrons extruded by atoms during ionization are further arrested by ions.Therefore, because of recombination, the ions emit their energy as photon emissions. Furthermore, because Sn atoms have high ionization energy(I.e. high ionization energy is required), Sn atoms have low ionization potential due to different atomic number.

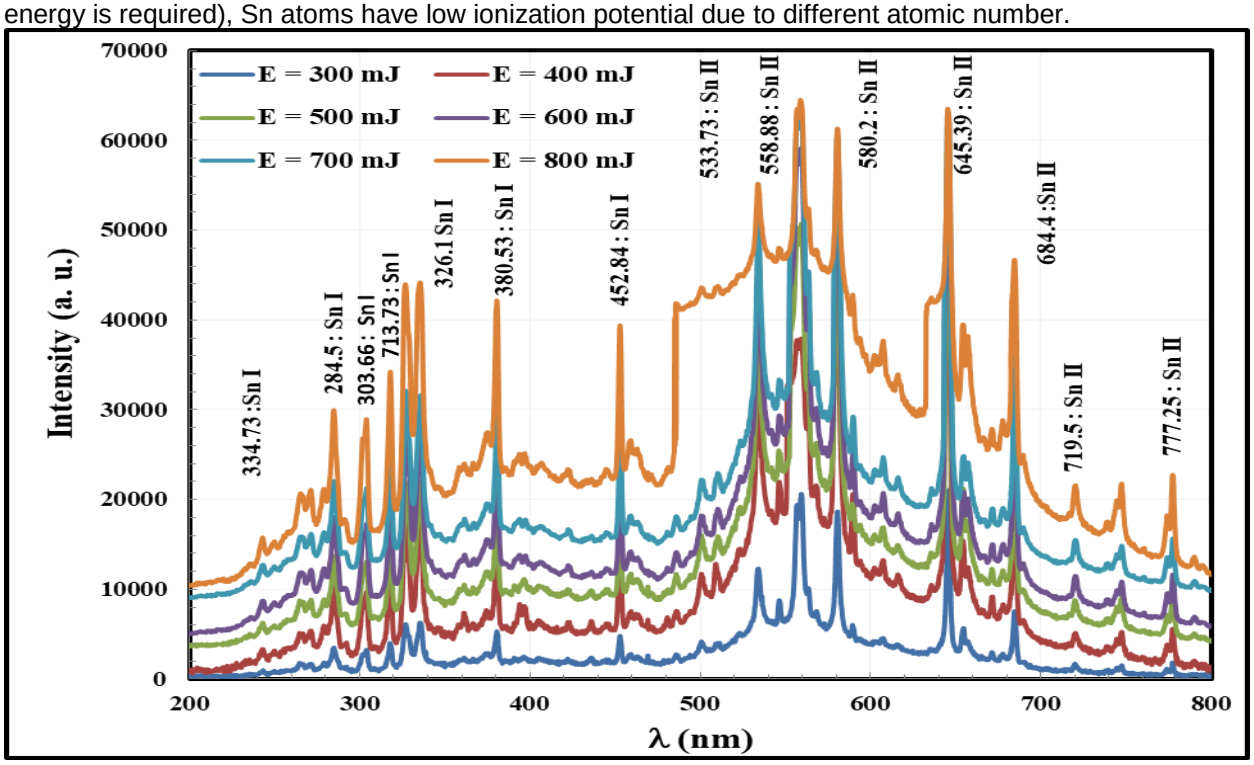

Fig -2Effect of laser energy (300-800)mJ on the Sn target at (200-100)nm

3-1-2 Zn plasma

Figure-3 displays the Zn plasma emission spectrum of varying pulse laser energies at a wavelength range of 200-1000 nm at ambient pressure in the air.From this figure, one can observe that there are several peaks of the neutral Zn I atom that occur in this spectrum at wavelengths 334.73 and 637 nm.At wavelengths of 277.81 , 481.4 , 492.73 , 611.12 , 758.83 and 777.69 nm, the ionic emission lines of Zn II appearThe strength of all the emission lines also increases with the increase in the pulsed laser energy to increase the mass density, the contrast increases, and the excitation increases. The overall strength of Zn I emission lines is far higher than that of Zn II, according to the findings shown in Figure-3.The Zn plasma emission spectrum revealed Zn to be more ionic than atomic Zn. The lower ionization energy of Zn atoms allows Zn atoms to ionize and thus causes Zn II emission lines to rise. It can be inferred, according to the findings in Figures-(2, 3), that the appearance of atomic and ionic elements in any elements in the target emission range depends on the ionization energy of the target atoms.

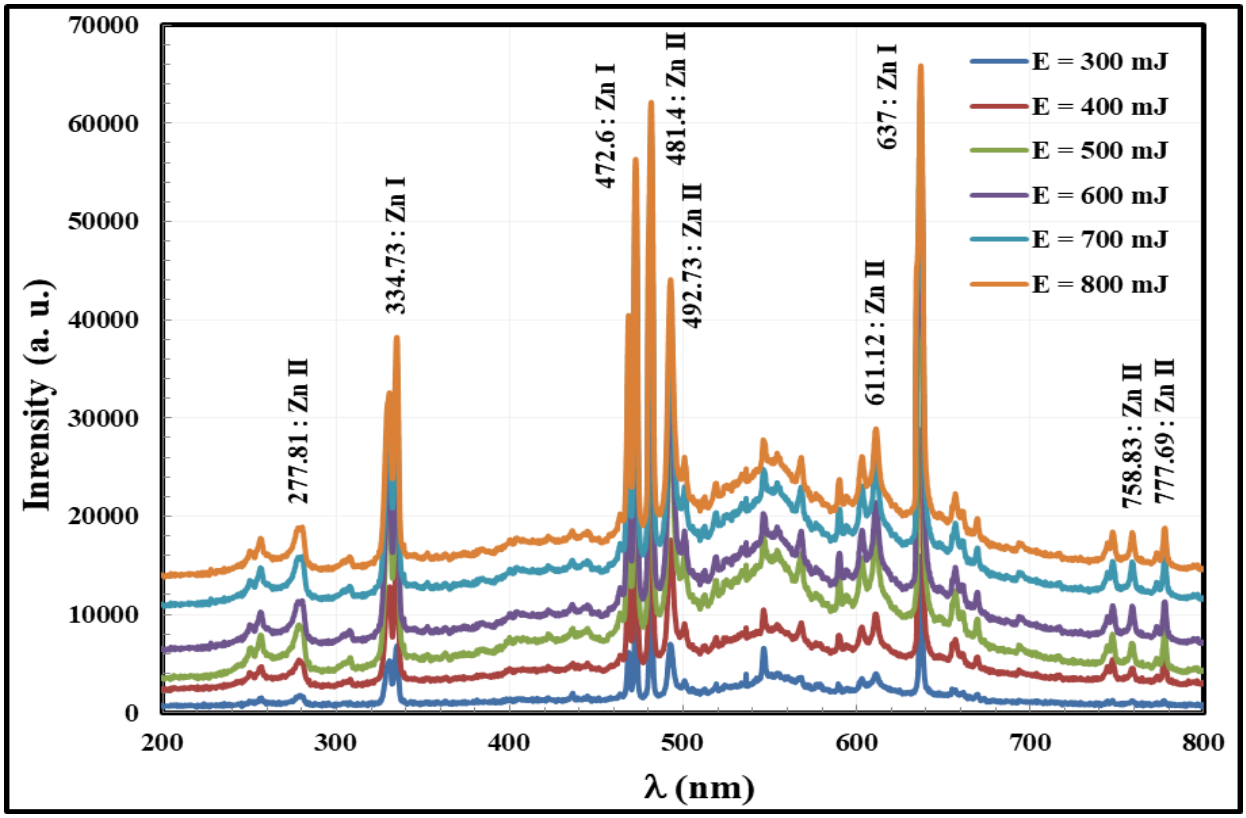

Fig-2 Effect of laser energy (300-800)mJ on the Zn target at (200-100)nm

3.2 Influence of Target Metal on the Electron Temperature

For Sn and Zn plasmas, the electron temperature (Te) emitted by lasers in the air at atmospheric pressure can be obtained from the tow line ratio equation (1).For the calculation of the electron temperature at varying laser energies, the atomic lines of Sn I and the ionic lines of Zn I elements are used (300, 400 ,500 ,600, 700 and 800 mJ). Table-1 and Table 2 tabulate the parameters of the Sn I and Zn I spectral lines. The electron temperature was measured and plotted in Figures-4 and 5 and using the data tabulated in Tables-1 and 2 and Equation (1).From this table, several characteristics can be noted, with increasing laser intensity, the electron temperature in both plasmas increases. This activity has been related to the transfer of laser thermal energy to electron kinetic energy due to increased forward peaking of laser energy of steady laser spot size [16].Under the same terms, the electron temperature value of Zn plasma is higher than that of Sn plasma.

3.3 Influence of Target Metal on the Electron Density

The effect of laser energy on the electron density of Zn and Sn target is measured and plotted in Figures-4 and 5, according to equations (2), Table-1 and 2.This figure shows that the number of electrons is inversely associated with the ionization energy of metal targets. Where the electron density of plasma would be greater for smaller the metal ionization potential mainly caused by the mass ablation and consequent denser vapor plasma plume creates higher electron density. With rising laser energy, the electron density of the two target plasma under study is increasing.In addition, the electron density of both plasmas increases with the rise in laser radiation, depending on the ionization energy. The absorption of laser photons in plasma by electron-neutral Inverse Bremsstrahlung can be due to this rise in electron density with increased laser intensity (IB).The excitation temperature and ionization temperature increase as the energy consumed increases, and so does the plasma's electron density.

Table 1-Spectroscopic parameters of Sn

Laser energy (mJ)	T_e (eV)	n_e*10^16 (cm^-3)	f_p(Hz) *10^{12}	λ_D *10^-3(cm)	N_d * 10^7
300	0.988	0.3	0.527	1.355	3.591
400	1.048	0.6	0.682	1.079	3.031
500	1.092	0.8	0.812	0.925	2.709
600	1.162	1.4	1.045	0.742	2.312
700	1.196	1.7	1.169	0.672	2.157
800	1.227	2.1	1.289	0.617	2.033

Table 2-Spectroscopic parameters of Zn

Laser energy (mJ)	T_e (eV)	n_e*10^19 (cm^-3)	f_p(Hz) *10^{13}	λ_D *10^-5(cm)	N_d * 10^6
300	1.927	2.1	4.091	2.438	1.260
400	1.944	2.2	4.192	2.390	1.247
500	1.977	2.4	4.381	2.306	1.223
600	2.000	2.5	4.517	2.250	1.207
700	2.038	2.8	4.738	2.165	1.183
800	2.110	3.3	5.178	2.016	1.141

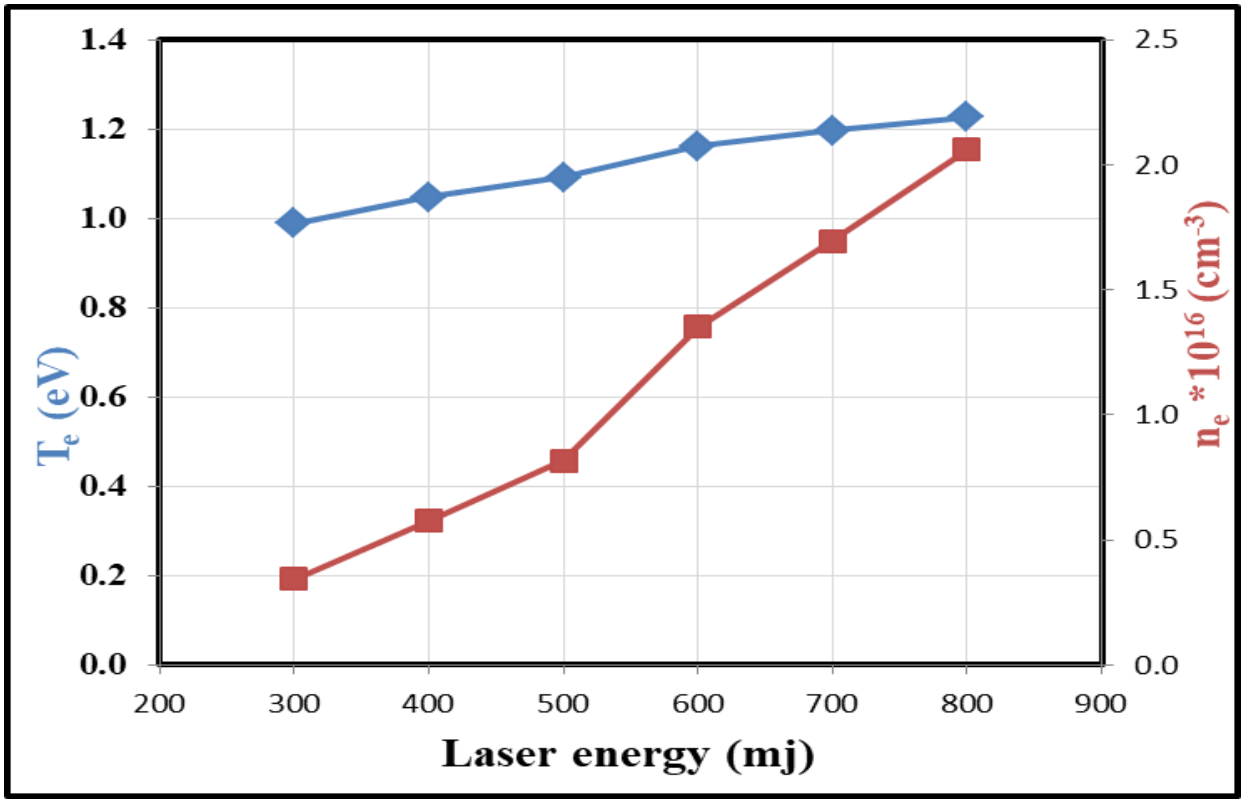

Fig- 4 The variation of electron temperature and electron density with laser energy in Sn at atmospheric pressure.

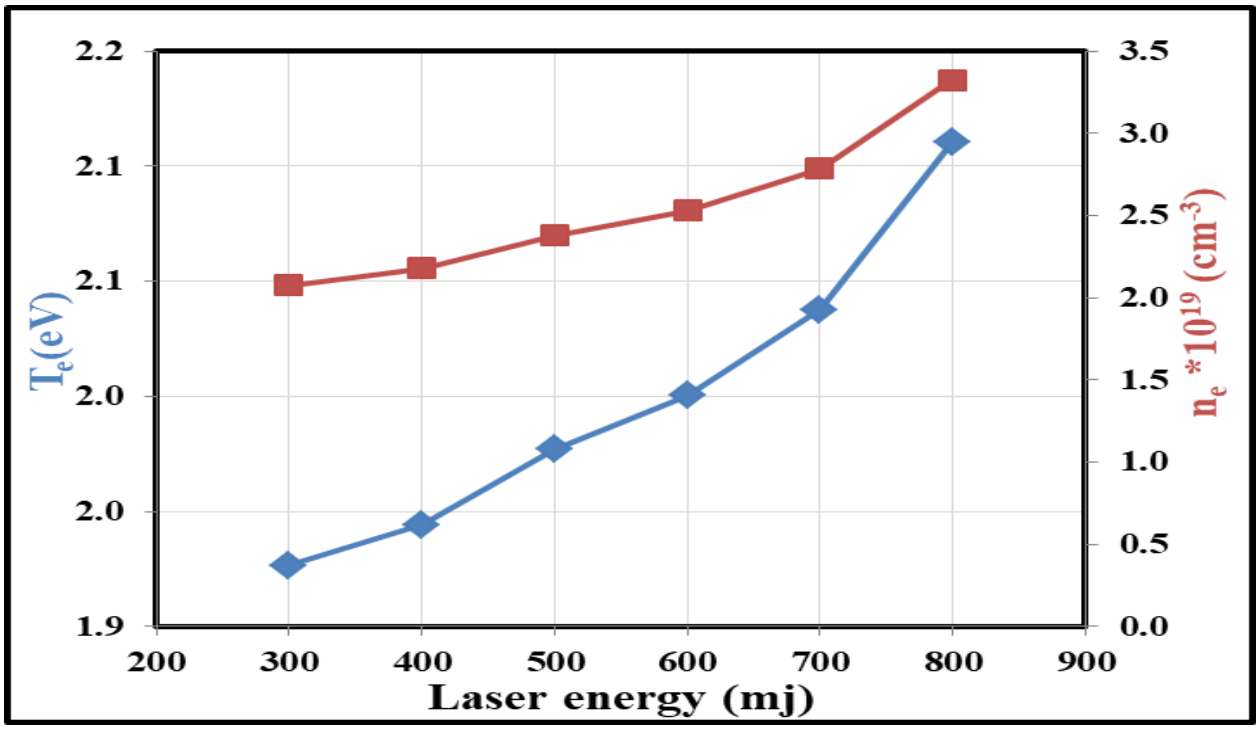

Figure-5 The variation of electron temperature and electron density with laser energy in Zn at atmospheric pressure.

3.4 Effect of Target Metal on the Plasma Frequency

The difference of the electron frequency with the laser energy of Zn and Sn plasmas is drawn in Figures-6 and 7 by the equation (4). Data points indicated an increase in plasma frequency with an increase in laser intensity for the two plasmas targets (Zn , Sn) in the figure-6 and 7.This behaviour is caused by an increase in the concentration of electrons, with an increase of laser intensity contributing to an increase in plasma frequency. The outcome also revealed that the plasma frequency value in Zn plasma is higher than that in Sn plasma. This effect was due to the fact that the concentration of electrons increased when the targets' ionization energy was reduced.

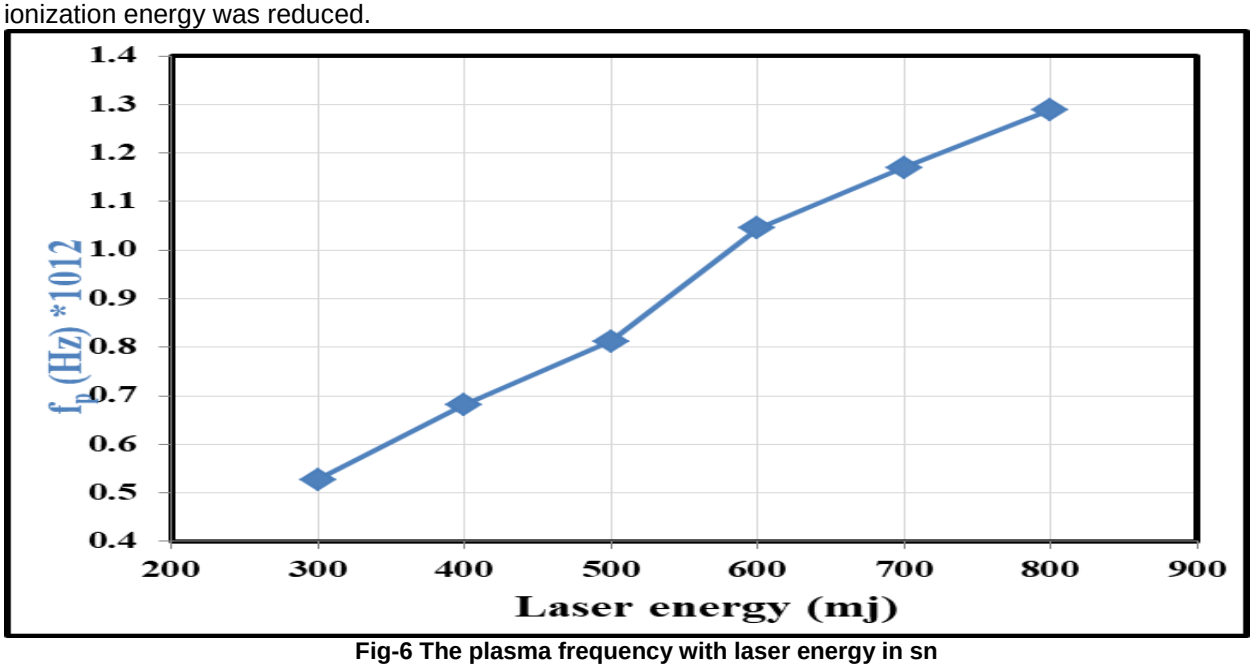

Fig-6 The plasma frequency with laser energy in sn

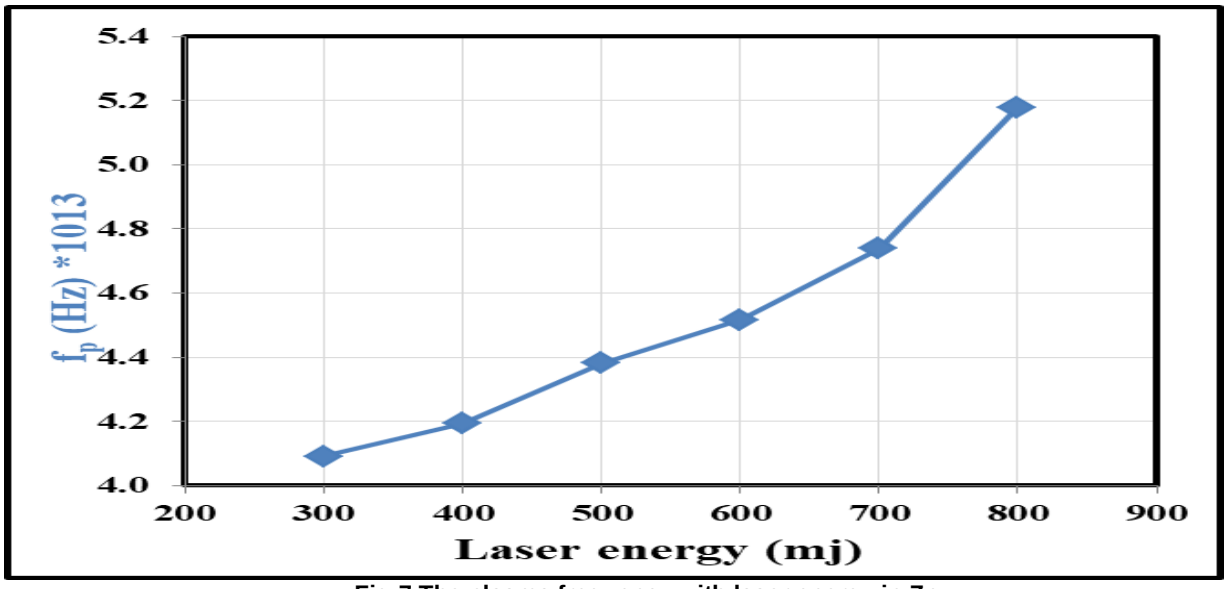

Fig-7 The plasma frequency with laser energy in Zn

3.5 Influence of Laser energy on the Debye Length and Plasma Parameter

In figure (8 and 9) explains the influence of laser energy on the duration of the Debye length and the plasma parameters measured by using equations (5) and (6), respectively. The data that calculated were tabulated in the Table-1.The findings revealed the length Debye and plasma parameters decreased as laser energy increased. The values of Debye length and plasma parameter of Sn plasma are greater than of Zn plasma. This behaviour of both parameters attributed to the fact that the electron density increase with decreasing of the ionization energy of the target atoms.

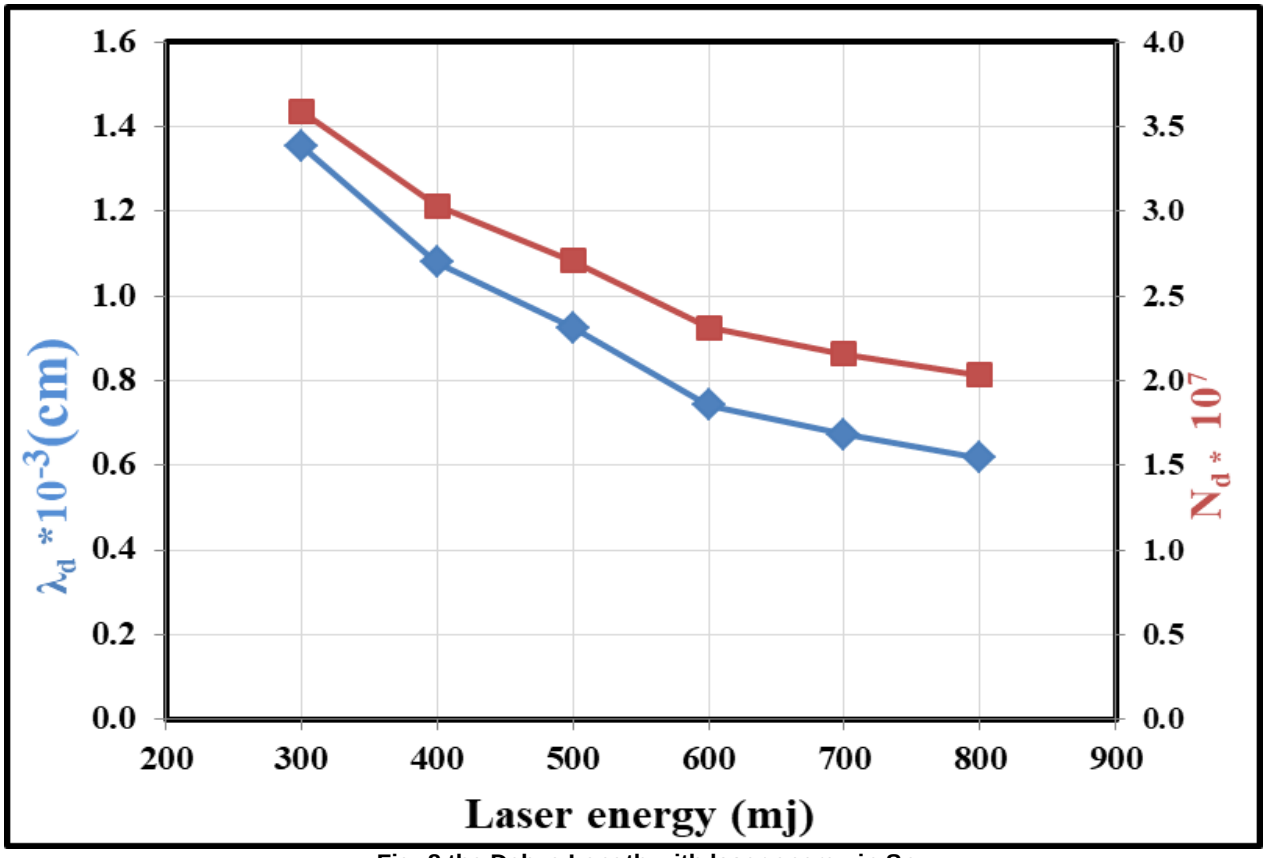

Fig- 8 the Debye Length with laser energy in Sn

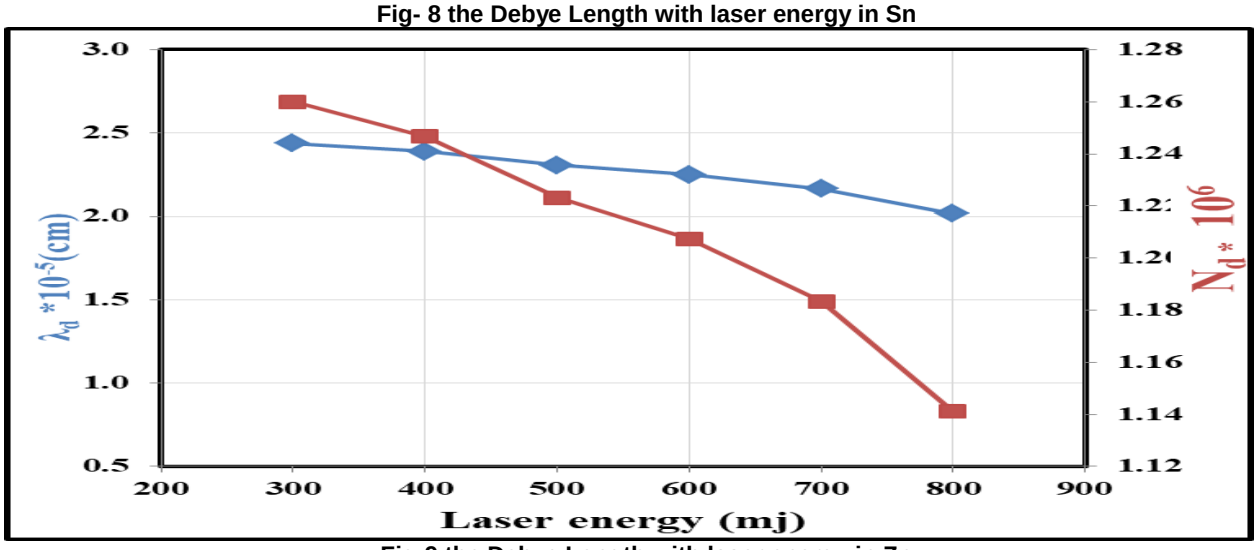

Fig-9 the Debye Length with laser energy in Zn

4. Conclusions

The effects of laser energy and the properties of a laser target on the absorption spectrum and plasma properties of Zn and Sn plasmas are illustrated in this review. The recent studies have shown that the increase in laser energy implies an increase in the strength of the emission line towards either target(Zn, Sn). The intensity of the atomic emission lines was even higher than that of the ionic lines. For any feature in the emission spectrum of the target, the presence of atomic and ionic emission lines depends on the ionization energy of the target atoms. Moreover, the properties of the plasma depend on the ionization energy of the target element and the laser energy also through this work, the difference between the electron density of Zn (3.3 * 1019) (cm-3) and Sn (2.1 * 1019) (cm-3), where The electron density is greater in Zn than in Sn, and so is the difference in electron temperature, which is directly proportional to the electron density of Zn (2.11 ev) Sn (1.22 ev). This difference is due to the different degrees of variation of the elements.

References

Abbas, Ahmed K, and Saif I. Muslim. “Measurement the Parameters of Cadmium Oxide Plasma Induced by Laser.” International Journal of Recent Research and Applied Studies 4, no. 10 (2017): 66–72.

Ahmed, Baida M. “Plasma Parameters Generated from Iron Spectral Lines by Using LIBS Technique.” IOP Conference Series: Materials Science and Engineering 928, no. 7 (2020). https://doi.org/10.1088/1757-899X/928/7/072096.

Ahmed, Baida M., Kadhim A. and Aadim, and Madyan A. Khalaf. “Verify the Plasma Parameters Generated from the Tin Material Using the Laser-Induced Plasma Technique.” World Scientific News 144, no. April (2020): 326–37.

Asamoah, Emmanuel, and Yao Hongbing. “Influence of Laser Energy on the Electron Temperature of a Laser-Induced Mg Plasma.” Applied Physics B: Lasers and Optics 123, no. 1 (2017): 1–6. https://doi.org/10.1007/s00340-016-6617-3.

Abbas, Qusay Adnan. “Effect of Target Properties on the Plasma Characteristics That Produced by Laser at Atmospheric Pressure.” Iraqi Journal of Science 60, no. 6 (2019): 1251–58. https://doi.org/10.24996/ijs.2019.60.6.8.

Haverkamp, J., R. M. Mayo, M. A. Bourham, J. Narayan, C. Jin, and G. Duscher. “Plasma Plume Characteristics and Properties of Pulsed Laser Deposited Diamond-like Carbon Films.” Journal of Applied Physics 93, no. 6 (2003): 3627–34. https://doi.org/10.1063/1.1555695.

Hanif, M., and M. Salik. “Optical Emission Studies of Sulphur Plasma Using Laser Induced Breakdown Spectroscopy.” Optics and Spectroscopy (English Translation of Optika i Spektroskopiya) 116, no. 2 (2014): 315–23. https://doi.org/10.1134/S0030400X1402009X.

Harilal, S. S., Beau O’Shay, Mark S. Tillack, and Manoj V. Mathew. “Spectroscopic Characterization of Laser-Induced Tin Plasma.” Journal of Applied Physics 98, no. 1 (2005): 1–7. https://doi.org/10.1063/1.1977200.

Harilal, S. S., C. V. Bindhu, Riju C. Issac, V. P.N. Nampoori, and C. P.G. Vallabhan. “Electron Density and Temperature Measurements in a Laser Produced Carbon Plasma.” Journal of Applied Physics 82, no. 5 (1997): 2140–46. https://doi.org/10.1063/1.366276.

Hameed, T. A., and S. J. Kadhem. “Plasma Diagnostic of Gliding Arc Discharge at Atmospheric Pressure.” Iraqi Journal of Science 60, no. 12 (2019): 2649–55. https://doi.org/10.24996/ijs.2019.60.12.14.

Khalaf, Madyan A., Baida M. Ahmed, and Kadhim A. Aadim. “Spectroscopic Analysis of CdO1-X: SnX Plasma Produced by Nd:YAG Laser.” Iraqi Journal of Science 61, no. 7 (2020): 1665–71. https://doi.org/10.24996/ijs.2020.61.7.15.

“National Institute of Standards and Technology (NIST) Atomic Spectra Database.,” 2019, 2019. https://dx.doi.org/10.18434/T4W30F.

Safeen, A., W. H. Shah, R. Khan, A. Shakeel, Y. Iqbal, G. Asghar, R. Khan, G. Khan, K. Safeen, and W. H. Shah. “Measurement of Plasma Parameters for Copper Using Laser Induced Breakdown Spectroscopy.” Digest Journal of Nanomaterials and Biostructures 14, no. 1 (2019): 29–35.

Unnikrishnan, V. K., KamleshAlti, V. B. Kartha, C. Santhosh, G. P. Gupta, and B. M. Suri. “Measurements of Plasma Temperature and Electron Density in Laser-Induced Copper Plasma by Time-Resolved Spectroscopy of Neutral Atom and Ion Emissions.” Pramana - Journal of Physics 74, no. 6 (2010): 983–93. https://doi.org/10.1007/s12043-010-0089-5.

Vera-Londoño, Liliana Patricia, Jaime Andrés Pérez-Taborda, and Henry Riascos-Landázuri. “Spectroscopic Analysis of Coal Plasma Emission Produced by Laser Ablation.” RevistaFacultad de Ingenieria 2016, no. 78 (2016): 69–72. https://doi.org/10.17533/udea.redin.n78a09.

Yueh, Fang Yu, HongboZheng, Jagdish P. Singh, and Shane Burgess. “Preliminary Evaluation of Laser-Induced Breakdown Spectroscopy for Tissue Classification.” SpectrochimicaActa - Part B Atomic Spectroscopy 64, no. 10 (2009): 1059–67. https://doi.org/10.1016/j.sab.2009.07.025.